



Article

Single-Particle ICP-MS/MS Application for Routine Screening of Nanoparticles Present in Powder-Based Facial Cosmetics

Deja Hebert ¹, Jenny Nelson ², Brooke N. Diehl ¹ and Phoebe Zito ^{1,*}

- Department of Chemistry, University of New Orleans, New Orleans, LA 70148, USA; dghebert@uno.edu (D.H.); bdiehl@uno.edu (B.N.D.)
- ² Agilent Technologies, Inc., 5301 Stevens Creek Blvd, Santa Clara, CA 95051, USA; jenny.nelson@agilent.com
- * Correspondence: pazito@uno.edu

Abstract: The short- and long-term impacts of nanoparticles (NPs) in consumer products are not fully understood. Current European Union (EU) regulations enforce transparency on products containing NPs in cosmetic formulations; however, those set by the U.S. Food and Drug Administration are lacking. This study demonstrates the potential of single-particle inductively coupled plasma tandem mass spectrometry (spICP-MS/MS) as a screening method for NPs present in powder-based facial cosmetics (herein referred to as FCs). A proposed spICP-MS/MS method is presented along with recommended criteria to confirm particle presence and particle detection thresholds in seven FCs. FC products of varying colors, market values, and applications were analyzed for the presence of Bi, Cr, Mg, Mn, Pb, Sn, Ag, Al, and Zn NPs based on their ingredient lists as well as those commonly used in cosmetic formulations. The presence of NPs smaller than 100 nm was observed in all FC samples, and no correlations with their presence and market value were observed. Here, we report qualitative and semi-quantitative results for seven FC samples ranging in color, brand, and shimmer.

Keywords: consumer care products; heavy metals; nanoparticles; regulations; consumer safety



Citation: Hebert, D.; Nelson, J.; Diehl, B.N.; Zito, P. Single-Particle ICP-MS/MS Application for Routine Screening of Nanoparticles Present in Powder-Based Facial Cosmetics. *Nanomaterials* **2023**, *13*, 2681. https://doi.org/10.3390/nano13192681

Academic Editors: Antonio R. Montoro Bustos and Pawel Pohl

Received: 14 August 2023 Revised: 26 September 2023 Accepted: 28 September 2023 Published: 30 September 2023



Copyright: © 2023 by the authors. Licensee MDPI, Basel, Switzerland. This article is an open access article distributed under the terms and conditions of the Creative Commons Attribution (CC BY) license (https://creativecommons.org/licenses/by/4.0/).

1. Introduction

Over 25 billion USD was generated in revenue by the U.S. cosmetic industry in 2021 due to increased consumer desire to improve their overall health and wellness. As a result, many cosmetic companies are now marketing their products with buzzwords such as vegan, naturally derived, eco-friendly, and cruelty-free [1] to target health-conscious consumers. This "clean beauty" marketing strategy originates from the push toward greener lifestyles and the use of environmentally safe and nontoxic products [2]. Despite their claims, clean beauty personal care products include potentially harmful chemicals, inadequate transparency on ingredient labels, and concealed substances. Cosmetic manufacturers use various ingredients to brand their products as convenient, long-lasting, and compatible with other skin applications. NPs are not the only dangerous ingredients added to FCs to enhance their physical and chemical properties. For example, cosmetics labeled as "wear-resistant" or "long-lasting" have been found to contain high concentrations of perand polyfluoroalkyl substances (PFAs) [3]. These findings, along with others, are focused on raising awareness of the use of chemicals in personal care products and disclosing their harmful effects to consumers [4–6].

Common additives in various cosmetic products include minerals, vegetable powders, oils, fats, dyes and pigments, preservatives, ultraviolet filters, water, solvents, and fragrances [7]. In the U.S., the Food and Drug Administration (FDA) has lenient labeling requirements for cosmetics with regard to the disclosure of these additives and chemicals. The main ingredients required to undergo FDA approval are color additives, which are defined by the FDA as "any dye, pigment, or other substance that can impart color to a cosmetic" [8]. While the FDA does not require premarket approval for most cosmetic

Nanomaterials **2023**, 13, 2681 2 of 17

ingredients, they have the ability to enforce the Fair Packaging and Labeling Act (FPLA) guidelines if there are notable health concerns with a product. The FPLA states, "Informed consumers are essential to the fair and efficient functioning of a free market economy" [9]. Metalss typically in the form of metal oxides, manganese dioxide (MnO₂), chromium oxide (CrO₃), magnesium oxide (MgO), aluminum oxide (Al₂O₃), silver (Ag), bismuth oxide (Bi₂O₃), and tin oxide (SnO₂) are commonly added to powder-based facial cosmetic products (herein referred to as FCs) to enhance shine, gloss, or sparkle and can act as absorbent or bulking materials [7]. To date, there are no regulations enforcing transparency on ingredient lists when it comes to the use of nanoparticles (NPs) in consumer care products.

NPs are operationally defined as particles smaller than 100 nm in size and are added to FCs to alter their physical and chemical properties, thereby enhancing their color, longevity, and quality [10,11]. In 2009, the cosmetic industry was one of the first to incorporate NPs in consumer care products, formulating over 13% of nanotechnology-based products [12]. Notably, titanium dioxide (TiO₂) and zinc oxide (ZnO) NPs are commonly used in sunscreen formulations as aerosols, powders, and liquids [13–15], potentially causing harmful effects to aquatic and human life. For example, TiO₂ and ZnO NPs have been identified as the primary cause of the destruction of entire coral reef colonies [16]. Other studies provide evidence that NPs may cross the epithelial barrier and risk toxicity to living organisms [17,18]. This paper highlights the need for transparency regarding the use of NPs in FC products, especially for health-conscious individuals who assume their clean beauty products are nontoxic, as some ingredients may lead to negative environmental and health impacts [19–21].

Despite reports on their harmful effects, the use of NPs in consumer care products, especially FCs, is not common knowledge to consumers, especially those advertised with buzzwords like vegan, nontoxic, organic, or natural. Further, the FDA does not enforce the disclosure of NPs on FC ingredient lists or the use of buzzwords that create the assumption that their products are safe and healthy. The lack of transparency regarding the use of NPs is problematic and a disservice to consumers who assume clean beauty products marked as vegan or nontoxic are safe to use. In 2022, the Science Advisory Board (SAB) of the Environmental Protection Agency (EPA) released a report entitled "Review of the EPA's Draft Fifth Contaminant Candidate List (CCL 5)" stating NPs were an emerging public health concern due to their unpredictable behavior and the overall lack of information regarding their persistence, reactivity, and short- and long-term impacts on human health and the environment [22].

All things considered, there is a large gap in the regulatory standards between the FDA and the EU on the use of nanoparticles in food and consumer care products. EU regulations enforce transparency on package labeling when NPs are added to cosmetic formulations [23]. This action prioritizes consumer awareness as to what cosmetic ingredients they are using on their bodies despite many unknown effects of NPs. Studies have shown that NPs enter aquatic environments through many sources including runoff, industrial applications and atmospheric deposition [24]. Once in the marine environment, NPs can move laterally and vertically, potentially adsorbing to organic matter [25–28], zooplankton [29,30], and other organisms [31].

Although numerous techniques are capable of characterizing inorganic NPs, few can disentangle NPs from other product ingredients due to their complex formulations. Other analyses to determine the size and distribution of NPs include microscopy, spectroscopy, and X-ray diffraction (XRD). However, these methods often require intense sample preparation and have low sample throughput. Previous approaches have utilized inductively coupled plasma—optical emission spectroscopy (ICP-OES) and inductively coupled plasma—mass spectrometry (ICP-MS) to detect and quantify bulk metal concentrations present in cosmetics [32–34]. However, studies focused on the presence, characterization, and size of NPs in FCs are lacking. Recently, the use of single-particle ICP-MS (spICP-MS) for NP detection in complex matrices has been reported [35–38]. In 2017, de la Calle et al. reported the use of spICP-MS for the screening of TiO₂ and Au NPs in cosmetic matrices

Nanomaterials **2023**, 13, 2681 3 of 17

including shampoos, sunscreens, creams, and toothpastes [39]. They also emphasized the importance of consumer awareness regarding the presence of NPs in cosmetics, further validating the need for methods to identify, quantify, and characterize NPs in complex formulations. In comparison to other analytical techniques, the application of spICP-MS/MS is a relatively simple, fast, and routine analysis to observe NPs present in FC products without the need for overcomplicated sample preparation. Additionally, the utilization of tandem mass spectrometry can reduce spectral overlap and improve the limits of detection [40].

The purpose of this study was to utilize single-particle tandem ICP-MS (spICP-MS/MS) as a comprehensive screening tool for detecting NPs in FCs. The information gained from this study will contribute to the literature regarding the need for transparency when using additives in consumer care products and the presence of NPs in cosmetics found in local U.S. stores that are not disclosed on the packaging labels, especially those claiming to be nontoxic. The method established in this study offers a quick screening tool to analyze FCs for the presence of NPs in complex cosmetic formulations.

2. Materials and Methods

2.1. Reagents

Multielement stock solutions were purchased from Agilent and Sigma-Aldrich (Sigma-Aldrich, St. Louis, MO, USA) and were prepared in 1% (v/v) trace-metal-grade HNO₃ (VWR, Radnor, PA, USA). Silver nanospheres (20, 50, 100, and 200 nm) suspended in sodium citrate were purchased from Nanocomposix (San Diego, CA, USA) as a reference material for single-particle size determination. Stock solutions of Ag nanospheres were diluted with nanopure water (Sartorius nanopure system, Göttingen, Germany) and prepared daily for analysis. Triton X-100 (1%) was used to prevent agglomeration and maximize the suspension of NPs present in the FC samples (Alpha Teknova, Hollister, CA, USA).

2.2. Cosmetics Selected for the Study

Several cosmetic samples, in the form of eyeshadows and facial powders, were purchased from local retailers in the United States. Products were purchased to obtain a range of low-end (low cost, \$) to high-end (high cost, \$\$\$) samples. The samples contained a range of colors and shade varieties such as matte shades, glitter shades, metallic shades, and shimmer shades. Overall, seven FCs were screened for the presence of NPs (five eyeshadows and two facial powders). Sample identification and descriptions are listed in Table 1.

Table 1. List of sample types, cost ranges,	and sample properties for	r each sample analyzed in
this study.		

Cosmetic Samples	Sample Type	Cost Range	Sample Properties
A	Eyeshadow	\$	Green, Shimmer
В	Eyeshadow	\$	White, Matte
С	Eyeshadow	\$\$	Maroon, Shimmer
D	Eyeshadow	\$\$	Deep Brown, Matte
E	Face Powder	\$\$	Pink, Shimmer
F	Eyeshadow	\$\$\$	Green, Matte
G	Face Powder	\$\$\$	Tan, Matte

2.3. Standard and Sample Preparation

Standard solutions: Calibration standards for single-particle analysis were prepared from multielement stock solutions. Standards were prepared daily and were serially diluted by volume to a final concentration of 1 μ g/L using a 1% solution of nitric acid as the diluent. The diluent was also used as the ionic blank for calibration.

Reference materials: The silver nanoparticle reference material was diluted to concentrations between 20 and $5250 \, \text{ng/L}$ with nanopure water as the diluent. Reference materials were agitated on a shaker and sonicated after dilution to ensure particle suspension and

Nanomaterials **2023**, 13, 2681 4 of 17

homogeneity. Four Ag reference standards (20, 50, 100, and 200 nm) were analyzed. The final concentration of each reference standard varied by size, with larger sizes requiring higher concentrations.

Sample Preparation: First, 0.1 g of each FC was dispersed into a 50 mL solution of 1% Triton X-100 in nanopure water. The samples were briefly shaken by hand before sonication in an ultrasonic bath for 2–3 min prior to analysis. The dilutions for each sample were made in the following ratios: 1:1, 1:3, 1:7, 1:15, 1:31, and 1:63. Each sample was shaken and sonicated in between each dilution. Samples were analyzed within 8 h of preparation to maximize particle suspension and stability.

Matrix Effect: In order to observe matrix effects, three solutions were prepared: (1) an unspiked FC sample, (2) a 1:1 dilution of an FC sample spiked with a known concentration of a 50 nm Ag NP reference material, and (3) a matrix-free reference material (RM). Each was suspended in 1% Triton X-100. Values for particle count, NPC, mass concentration, and mean size were averaged between five injections (n = 5). Recovery percentages were calculated based on the % recovered in the spiked sample versus the RM.

2.4. Instrumentation

An Agilent 8900 ICP-MS/MS (Agilent Technologies, Santa Clara, CA, USA) equipped with nickel sampling and skimmer cones, a concentric glass nebulizer, a quartz spray chamber, and a 1.0 mm quartz torch was operated in single-particle mode. The instrument was tuned daily to optimize sensitivity. Masshunter software (Version 5.2) was used for all ICP-MS/MS analyses and data curation. The operational parameters for the analysis can be found in Table 2. Analyses were performed measuring the monitored masses (Table 2) in Time-Resolved Analysis (TRA) mode. During tandem MS, helium gas mode was utilized and both quadrupoles were set to the indicated monitored mass for on-mass measurements. The nebulization efficiency was calculated by the instrument software to obtain accurate NP sizes and elemental compositions. The nebulization efficiency is the amount of analyte that enters the plasma in relation to the amount of analyte delivered to the nebulizer. For this study, the nebulization efficiency was calculated using the Ag reference material, maintaining a value of 0.06–0.065, or 6–6.5%. The calculation was based on the particle frequency method established by Pace et al. [41].

Table 2. Operational parameters of the study.

Parameter	No Gas	Helium
Scan Mode	SQ	MS/MS
Gas Flow (mL/min)	0	1.0
Elements (Monitored Mass)	Al (27), Pb (208), Ag (107), Bi (209)	Mn (55), Zn (66), Cr (52), Mg (24), Sn (118)
RF Power (W)	_	1600
Sampling Depth (mm)		10
Carrier Gas (L/min)		1.20
Dwell Time (ms)		0.1

Particle diameter was calculated by the software, which assumed particles were spherical in nature and had a specified chemical composition. The particle density and mass fraction formula of the assumed chemical composition were dependent on the particle diameter and affected the size distribution. The assumed chemical compositions in this study were chosen based on common cosmetic ingredients as well as the ingredients listed on the product packaging of the chosen samples. The assumed chemical compositions are listed in Table 3, along with their respective particle densities and mass fractions.

Nanomaterials **2023**, 13, 2681 5 of 17

Table 3. Assumed chemical compositions for each NP type identified in this study. The mass fraction and particle density entered into the software for size calculations are listed for each NP composition. Values for NP density were obtained from the literature [42].

NP ID	Assumed NP Composition	Mass Fraction	NP Density (g/cm ³)
Mn	MnO_2	0.744	5.03
Zn	ZnO	0.800	5.60
Cr	Cr_2O_3	0.342	5.22
Mg	MgO	0.603	3.60
Al	Al_2O_3	0.265	3.97
Pb	PbO	0.928	9.64
Ag	Ag	1.000	10.50
Bi	Bi_2O_3	0.448	8.90
Sn	SnO_2	0.788	6.85

2.5. Transmission Electron Microscopy

A random sample was selected to confirm the presence of NPs in the FCs using transmission electron microscopy (TEM) to complement the spICP-MS/MS data. Sample G was dispersed in 200-proof ethanol at a concentration of 2.5 mg/mL, prepared on a Lacey/Carbon 200-mesh copper grid, and evaporated overnight. TEM images were obtained on a JEOL 2010 equipped with an EDAX genesis energy-dispersive spectroscopy (EDS) system operating at an accelerating voltage of 200 kV with an emission current of $109~\mu A$. Figure S9 illustrates the presence of nanoparticles smaller than 100~nm.

2.6. Baseline and Particle Detection Threshold Determination

Masshunter determined the particle baseline (Y_B) automatically using a proprietary algorithm. The diluent (1% Triton x-100) was used as a blank. Three replicates of the blank were analyzed, and the mean intensity values for the three runs were averaged for each element. In cases where the software determined that the baseline for the samples was lower than the baseline calculated for the blank, the baseline was manually adjusted to Nanomaterials 2023, 13, x FOR PEER REQUEINTHE calculated mean intensity value of the blank (Figure 1). This was performed in all effort to minimize false positives so that signal intensities lower than the baseline observed in the blank were not considered as particle events.

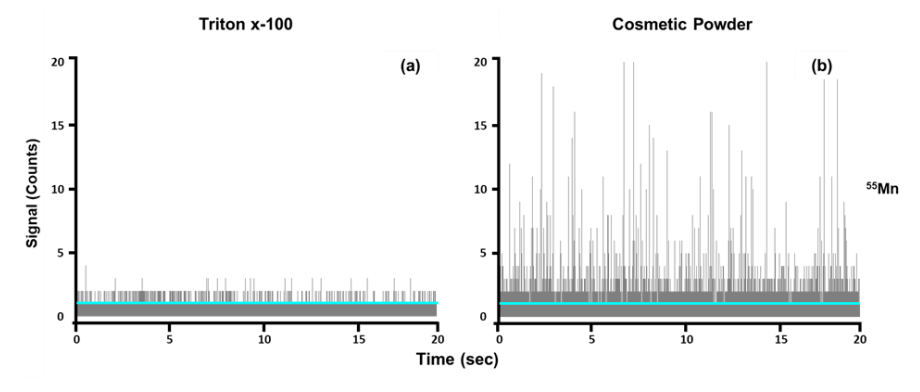


Figure 1. Time scans are shown formanganese (a) The 4% Tritoton-1000 suded the liberal asked was perpentially extensively with the liberal asked was perpentially extensively with the blue line indicating the baseline in the same position as the mean intensity determined for the blank.

A challenge that must be considered in single periodic adjust sixthe threspose of particles like thankly represented in the considerable of the co

 $N_B + 2.33\sqrt{N_B} \tag{1}$

(100)110

Nanomaterials **2023**, 13, 2681 6 of 17

(N_B) (Equation (1)). Particles were confirmed when the number of particles detected in the sample exceeded the value calculated using Equation (1) [43]:

$$N_B + 2.33\sqrt{N_B}$$
 (1)

Once the baseline was established and the presence of particles had been confirmed, two particle detection thresholds were calculated for each element in each sample based on Equations (2)–(5). These particle detection threshold calculations were specifically established for microsecond dwell time spICP-MS in samples with high background [44]. This technique was later applied by Vidmar et al. for the screening of nanoparticles in food matrices [35]. Thresholds I (Equation (2)) and II (Equation (3)) are considered "critical values", where Threshold I is applied to baselines higher than five counts and Threshold II is applied to baselines lower than five counts. In calculations of Threshold I and II, only errors related to the detection of false positives are considered. Thresholds III (Equation (4)) and IV (Equation (5)) are considered "detection values" and are applied to baselines higher than five counts and lower than five counts, respectively. A more conservative approach is taken when calculating Thresholds III and IV, which account for both false positives and negatives [44].

$$Y_{\rm B} + 1.64\sqrt{Y_{\rm B}}$$
 (2)

$$Y_B + 2.33\sqrt{Y_B}$$
 (3)

$$Y_{B} + 2.71 + 3.29\sqrt{Y_{B}} \tag{4}$$

$$Y_B + 2.71 + 4.65\sqrt{Y_B}$$
 (5)

Although the software determined a particle detection threshold, this value could be manually inputted based on user preference. In this case, all particle detection thresholds REVIEW were entered manually to maintain consistent data treatment. The placement of Threshold I and Threshold III are illustrated as a representative time scan (Figure 2a) and signal distribution plot (Figure 2b) for Cr NPs detected in FCs. The signal distribution plot was anslated from the time scan.

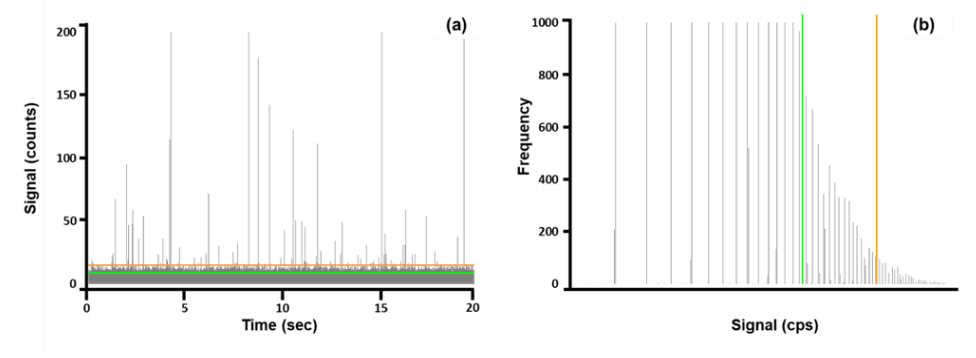


Figure 2: A representative time scan (a) and signal distribution plot (b) are shown for chromium present in one of the seven analyzed cosmetic samples. The green line indicates the "critical value threshold" (Threshold II), and the orange line indicates the "detection value" threshold (Threshold IIII). Thresholds were calculated based on Equations (2) and (4) because the determined baseline in this sample was higher than five counts.

The number of particles, limit of detection (LOD) size, and most frequent size were determined after manually entering the particle detection thresholds into the Masshunter software. Values for the calculated thresholds presented in Figure 2 are listed in Table 4.

Table 4. The number of particles, LOD_{size} , and most frequent size are shown for the thresholds presented in Figure 2.

Threshold	Number of Particles	LODsize (nm)	Most Frequent Size (nm)	
1	6255	35	38	
0	1005	40	4.6	

Nanomaterials **2023**, 13, 2681 7 of 17

Table 4. The number of particles, LOD_{size}, and most frequent size are shown for the thresholds presented in Figure 2.

Threshold	Number of Particles	LOD _{size} (nm)	Most Frequent Size (nm)
1	6255	35	38
3	1225	43	46

3. Results and Discussion

3.1. spICP-MS/MS as a Screening Method for Nanoparticles in Powder-Based Facial Cosmetics

When analyzing data after an spICP-MS/MS analysis, step 1 is to confirm if particles are present in the sample. The confirmation of particle presence in spICP-MS has been referred to as "screening" in the literature [43]. Seven FC samples were screened for the presence of nine elements (Table 5), some of them disclosed on the product ingredient lists as metal oxides as well as a few commonly found in FCs. Out of the seven FC samples, only two did not contain Bi. Time scans for each element in the seven samples can be found in the Supplementary Information (Figures S1–S7), as well as time scans for each element in the blank (Figure S8).

Table 5. Screening results of seven cosmetic samples for nine metal particle types.

Particle Type	Number of Samples
Mn	7
Zn	7
Cr	7
Mg	7
Al	7
Pb	7
Ag	7
Bi	5
Sn	7

3.2. spICP-MS/MS for Size Distributions

A simple screening for particles can be accomplished through a fast routine analysis, as presented in this study. However, caution must be used during data processing to ensure confidence in the determined size distributions. Microsecond dwell times and complex sample matrices are internal and external factors, respectively, that create ambiguity in the measurements. When using microsecond dwell times, multiple readings are made per particle, and those readings make up a single particle event, resulting in the calculation of a peak area [45]. Under these circumstances, the particle events are peaks rather than simple pulses. Accordingly, "pulse events" falling under the applied threshold value are eliminated from any size distribution calculations as opposed to "peak events" that are reduced in intensity based on where the threshold is applied [46]. As a result, the overall particle size distribution may be unknowingly shifted to larger sizes. Furthermore, the high complexity of the sample matrix presents a high dissolved background (Figure 2a in grey), effectively increasing the baseline, making smaller particles indistinguishable. This also causes an erroneous shift to larger particle size distributions. When this occurs, the size distribution results should be considered as "partial" unless a complementary technique is used to confirm the size distribution.

Despite not obtaining full size distributions, size data obtained using this approach are practical for screening NPs present in FCs. Here, we provide a semi-quantitative approach using spICP-MS/MS to acquire mode particle diameters for particles present in FC products, confirming that particles exist in a sample at that size or greater. Any observations of NPs present in FCs are a testament to the applicability of this method as a screening tool, especially to satisfy criteria set by EU regulations for NPs. To minimize random error due to Poisson statistics and any bias stemming from multiple particle events,

D

Nanomaterials **2023**, 13, 2681 8 of 17

 $\overline{\mathbf{R}}$

_		A	Ъ	C	D	
Element ID	Mode Diameter (nm)	NPC (cles	parnode particle diarograms are only Part Diamoutte below 200 are m /L) above 2000 are mark etes (b) (about the critical value calculated using	ove the limit of quants	ots that fall between 2000 of 2000 in the standard parties of the second standard parties of the second sec	i- ^M Dia
Mn		BLQ	diameter 5(a re repor 4 ¢ 7 x t 110 ² m	ore conservative705the	11070 applied thresAdlO to limit	
Zn]	BLQ			s) calculated by the software are tilation of the NPC is based on a	
Cr		BLQ	formula reporte BleS where [41].	4.5 x	10^7 56 1.1×10^8	
Mg	_	ALQ			en FCs using spICP-MS/MS are 108 was found to be ALQ in all sam-	
Pb		BLQ			110 wsed in commetic for 10 laxi 10 s	
Ag]	BLQ			ent or opacifying agent" and has The amounts of Ag NPs present in	
Bi		ND			சுற்கince they are address antimi-	
Sn	66	4.6 x	crobial agents in trace concentrate 10 ⁷ in FC products varied actors sam	tions [48]. Overall, the paper is the paper	presence and size of NPs detected 107 rket price value. In consideration	
Al	_	ALQ	of EU regulations at least one e	lement in pa xticle form	was observed below 160 nm for	
			Samples A=G (Figure 3). Sample BLO=Tology limit of guard	titation: particle cou	nt (\$\$), and sample A, a low-cost nt < 200 ALO = above limit o Nos respectively. However, it o	of quar

eyeshadow (S), had the highest and lowest Humbers of NPs, respectively. However, for results marked as WLQ, Hotther safely edilutions could be performed to confirm whether the confirmed particles meet the operational definition of NPs. For results listed as BLQ, it is possible to analyze these samples at higher concentrations to increase the number of particle events. However, at such high concentrations, the background can increase, prompting the need for further sample manipulation to decrease the matrix effects, which increases the subjectivity in the measurements. None of the product packaging for the FC samples (A–G) identified any of the ingredients as being nanosized, as this is not regulated in the U.S., emphasizing that further transparency should be provided to consumers.

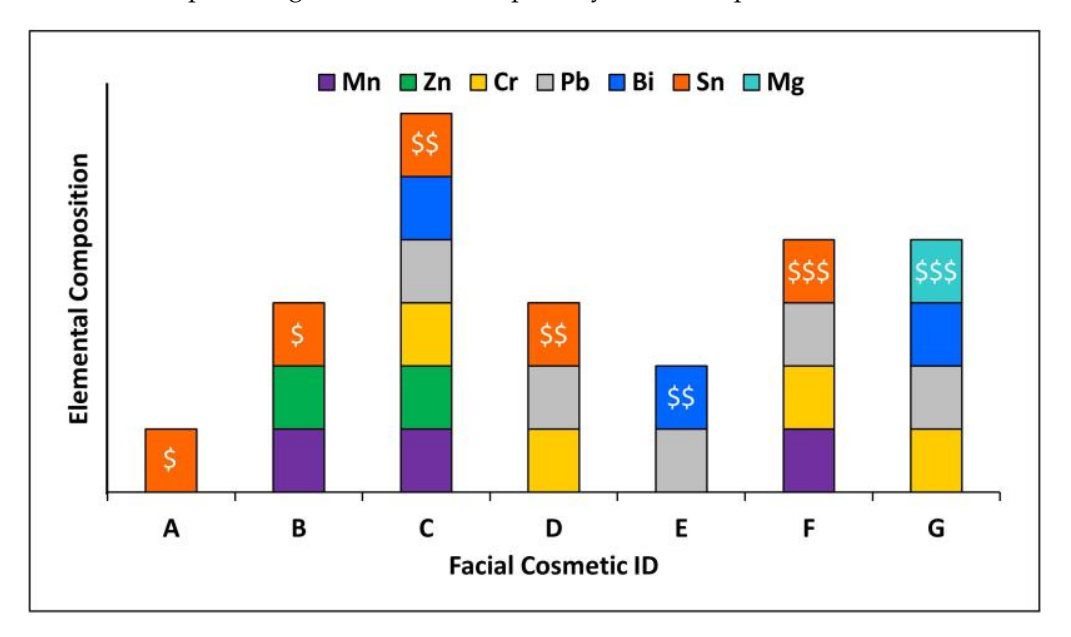


Figure 1-explainment abstraction positions of spotential 0 or 0 and 0 and 0 and 0 and 0 are 0 and 0 and 0 are 0 are 0 are 0 are 0 are 0 are 0 and 0 are 0 and 0 are 0 a

3.3. Addressing Spectral Interferences

ICP-MS continues to be a reliable technique for elemental analysis. No potential challenge is the presence of spectral interferences. Spectral over analysis can come as a result of isobaric interferences, two elements with the mass, or polyatomic interferences, the presence of a polyatomic ion with as the measured element. Collision/reaction cell (CRC) technology has been a way to combat these spectral interferences [40,49–51]. Even further, who

Nanomaterials **2023**, 13, 2681 9 of 17

Table 6. Semi-quantitative results for particles present in seven FC samples labeled A–G.

	I	A		В		C		D		E		F	(3
Element ID	Mode Diameter (nm)	NPC (Particles/L)	Mode Diameter (nm)	NPC (Particles/L)	Mode Diameter (nm)	NPC (Particles/L)	Mode Diameter (nm)	NPC (Particles/L)	Mode Diameter (nm)	NPC (Parti- cles/L)	Mode Diameter (nm)	NPC (Par- ticles/L)	Mode Diameter (nm)	NPC (Parti- cles/L)
Mn	Bl	LQ	50	4.7×10^{7}	62	7.5×10^{7}	Α	LQ	50	3.1×10^{7}	A	LQ	BI	.Q
Zn		ĹQ	96	3.1×10^{7}	100	9.8×10^{7}	Е	BLQ]	BLQ	116	1.1×10^{8}		LQ
Cr	Bl	LQ	В	BLQ	56	4.5×10^{7}	56	1.1×10^8	50	1.8×10^{8}	B	LQ	52	8.5×10^{7}
Mg	A	LQ	A	LQ	114	1.3×10^{8}	120	2.6×10^8	1	ALQ	A	LQ	92	2.0×10^{8}
Pb	Bl	LQ	В	BLQ	30	1.1×10^{8}	30	1.0×10^8	20	7.5×10^{7}	20	4.6×10^{7}	20	9.2×10^{7}
Ag	Bl	ĹQ	В	BLQ	B	LQ	Е	SLQ]	BLQ	Bl	LQ	BI	LQ
Bi	N	ID	1	ND	12	4.2×10^{7}		LQ.]	BLQ	14	2.9×10^{7}	14	3.2×10^{7}
Sn	66	4.6×10^{7}	58	5.9×10^{7}	68	5.1×10^{7}	72	2.9×10^{7}	66	2.3×10^{8}	B	LQ	BI	LQ
Al	A	LQ	A	LQ	A	LQ	A	LQ	I	ALQ	A	LQ	Al	LQ

 $BLQ = below \ limit \ of \ quantitation; \ particle \ count < 200. \ ALQ = above \ limit \ of \ quantitation; \ particle \ count > 2000. \ ND = not \ detected.$

Nanomaterials **2023**, *13*, 2681 10 of 17

3.3. Addressing Spectral Interferences

ICP-MS continues to be a reliable technique for elemental analysis. Nonetheless, one potential challenge is the presence of spectral interferences. Spectral overlap in ICP-MS analysis can come as a result of isobaric interferences, two elements with the same isotopic mass, or polyatomic interferences, the presence of a polyatomic ion with the same mass as the measured element. Collision/reaction cell (CRC) technology has been introduced as a way to combat these spectral interferences [40,49–51]. Even further, when applied to a tandem mass spectrometry system, levels of sensitivity can increase significantly [52–54]. This combination is extremely advantageous when considering the need for elemental analysis in high-matrix samples (i.e., environmental, biological, and food) where spectral interferences are highly probable.

Though the use of CRC technology has proven to be an effective approach to overcoming spectral interferences in normal ICP-MS analysis, its use in the single-particle mode has not been examined as extensively. Two options are available when utilizing CRC technology. The first option is the introduction of a collision gas that eliminates polyatomic interferences via kinetic energy discrimination (KED). The second option is the introduction of a reaction gas that can either react with the polyatomic interferences, which will then be filtered out by the final quadrupole, or react with the analyte ions to form an adduct ion that can be measured in "mass-shift" mode. The use of helium as a collision gas for spICP-MS measurements has been reported with demonstrated repeatability and an increase in size detection limits by 10–15% when compared with the no-gas mode [55]. The increase in size detection limits is undesirable; however, the measurement of particle types with severe spectral interferences may only be possible with the use of a collision or reaction gas. In addition, Bolea-Fernandez et al. reported on the use of different reaction gases (H₂ (onmass) and NH₃ (mass-shift)) for single-particle measurements of Fe₃O₄ nanoparticles [56]. The results from this study revealed that the use of a heavier reaction gas like NH₃ can induce significant peak broadening compared to lighter cell gases like H₂ and He, leading to higher size detection limits and inaccurate size distributions. A thorough explanation of this phenomenon can be found in the referenced study [56].

In this study, there were no isobaric interferences. Common polyatomic interferences for each element are listed in Table 7 and can be found in the literature [57]. Of the possible polyatomic ions listed, those reported for Ag, Sn, Pb, and Bi seem unlikely to pose major interferences considering the sample matrix. The remaining elements (Mg, Al, Cr, Mn, and Zn) are prone to a higher number of more probable polyatomic interferences.

Element	Possible Interferences
²⁴ Mg	¹² C ₂ +
²⁷ Al	$^{12}C^{\bar{15}}N^{+}$, $^{13}C^{14}N^{+}$, $^{14}N^{2}$ spread, $^{1}H^{12}C^{14}N^{+}$
⁵² Cr	$^{35}\text{Cl}^{16}\text{O}^{1}\text{H}^{+}$, $^{40}\text{Ar}^{12}\text{C}^{+}$, $^{36}\text{Ar}^{16}\text{O}^{+}$, $^{37}\text{Cl}^{15}\text{N}^{+}$, $^{34}\text{S}^{18}\text{O}^{+}$, $^{36}\text{S}^{16}\text{O}^{+}$, $^{38}\text{Ar}^{14}\text{N}^{+}$, $^{36}\text{Ar}^{15}\text{N}^{1}\text{H}^{+}$, $^{35}\text{Cl}^{17}\text{O}^{+}$
⁵⁵ Mn	$^{40}Ar^{14}N^{1}H^{+}$, $^{39}K^{16}O^{+}$, $^{37}Cl^{18}O^{+}$, $^{40}Ar^{15}N^{+}$, $^{38}Ar^{17}O^{+}$, $^{36}Ar^{18}O^{1}H^{+}$, $^{38}Ar^{16}O^{1}H^{+}$, $^{37}Cl^{17}O^{1}H^{+}$, $^{23}Na^{32}S^{+}$, $^{36}Ar^{19}F^{+}$
⁶⁶ Zn	$^{50}\mathrm{Ti}^{16}\mathrm{O}^{+}$, $^{34}\mathrm{S}^{16}\mathrm{O}_{2}^{+}$, $^{33}\mathrm{S}^{16}\mathrm{O}_{2}^{1}\mathrm{H}^{+}$, $^{32}\mathrm{S}^{16}\mathrm{O}^{18}\mathrm{O}^{+}$, $^{32}\mathrm{S}^{17}\mathrm{O}^{2+}$, $^{33}\mathrm{S}^{16}\mathrm{O}^{17}\mathrm{O}^{+}$, $^{32}\mathrm{S}^{34}\mathrm{S}^{+}$, $^{33}\mathrm{S}_{2}^{+}$
107 Ag	$^{91}{ m Zr^{16}O^{+}}$
¹¹⁸ Sn	102 Ru 16 O ⁺ , 102 Pd 16 O ⁺
²⁰⁸ Pb	¹⁹² Pt ¹⁶ O+
²⁰⁹ Bi	$^{193}\mathrm{Ir^{16}O^{+}}$

To examine the effects of different CRC gases, a single cosmetic sample was analyzed in three different gas modes: O_2 mass-shift, NH_3 mass-shift, and He on-mass. The elements analyzed were limited to Mg, Al, Cr, Mn, and Zn, as they are most likely to suffer from polyatomic interferences. To assess the effects of the three cell gases, the software-determined baselines were compared to determine their ability to decrease background presence. In addition, size detection limits (LOD_{size}) were calculated for each element in the different gas modes based on the Threshold III and IV calculations described above. These values

13, x FOR PEER REVIEW 11 of 17

Nanomaterials **2023**, 13, 2681 11 of 17

Table 8. Comparison of baselines and size detection limits obtained for four elements suffering polare presented in Table 8. Though Zn was analyzed, the Zn in this sample appeared to yatomic interferences in three gas modes. Scans with no particle signal are indicated by "NPS".

"NPS". therefore, values for Zn are not included.

	He		Table 8	NH3 Comparison	of baselines and	$ m \frac{O_2}{nd\ size\ detection\ limits\ obtained\ for\ four\ elements\ suffering$			
seline	LOD_{size}				ces Mass ee diffe				
(cps)	(nm)	(cps)	by "NPS	″(nm)	Shift	(cps)	(nm)	Shift	_
11773 -	125	6303 He		225	$24 \rightarrow 41$ NH ₃	82259	148	24 0 40	
.8577 .6441	Elemen§9 — ID 42	7871	LOD _{size} (nm)	92 Baseline N/A (cps)		97827 2Mass Shift 28047	96 Baseline (54 s)	27 43 10D _{size} 52mh)68	Mass Shift
6044	²⁴ Mg48	111,773 NPS	125	N/A 6303	55 → 72≥5	3 46 2→ 41	8 6,4 59	551 4 871	24 o 40
	²⁷ Al ⁵² Cr ⁵⁵ Mn	48,577 46,441 6044	69 42 48	7871 NPS NPS	92 N/A N/A	$\begin{array}{c} 27 \rightarrow 44 \\ 52 \rightarrow 69 \\ 55 \rightarrow 72 \end{array}$	97,827 28,047 3462	96 54 64	$ \begin{array}{c} 27 \rightarrow 43 \\ 52 \rightarrow 68 \\ 55 \rightarrow 71 \end{array} $

While it is true that polyatomic interferences may contribute to an elevated background, comparing baselime interference that the interference transmining three optimal evated background. The dataginulable optimal baselines realizes the dataginulable optimal reaction gas; howevers protected by the object of the lower statistic optimal between the comparing the lower statistic optimal between the comparing the LOD result of the lower statistic optimal intersities to be the protection of the lower statistic optimal intersities to be the comparing the LOD result of the lower statistic optimal intersities to be the protection of the lower statistic optimal intersities to be the protection of the lower statistic optimal intersities to be provided in the He gas mode despite the typically higher baseline values, the lowest values were observed in the He gas mode despite the typically higher baseline values. The reason for this, as previously mentioned, may may be peak broadening when using heavier reaction gases like NH3 and Or An example of of increased peak windrasped peak when using heavier reaction gases like NH3 and Or An example of of increased peak windrasped peak when a sharpeward peak observed in seigent a figure 4a.

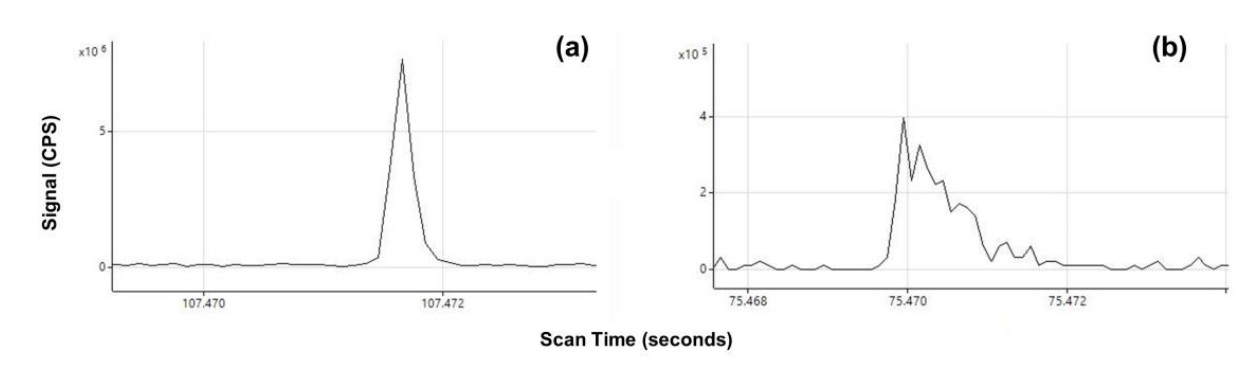


Figure 4. A single observed peak is shown for a magnesium particle analyzed in (a) He gas mode and (b) NH₃ mass-shift mode. The peak observed in (b) exhibits increased peak width and poor peak shape.

The use of collision and reaction cell gases has proven to be an effective measure. The use of collisions and certified real gases has proven to be an effective measure. The use of collisions and certified real gases has proven to be an effective measure. The use of collisions and certified gases in the collisions are considered to the collisions and collisions are collisions and collisions are collisions as observed however, the use of inchain collisions are collisions as observed in this study. Therefore, without satisficing peak shape, peak width, and signal intensity. spectral interferences without sacrificing peak shape, peak width, and signal intensity.

3.4. Importance of Dilution

3.4. Importance of Dilution It is suggested when conducting a single-particle analysis to evaluate several dilution factors, especially for samples with complex matrices. There are a number of reasons why It is suggested when conducting a single-particle analysis to evaluate several dilution factors, especially for from the levil background, factors, especially for from the levil bring matrices background sample this can be beneficially for the proper dilution of flutors ample and so when measuring an unknown sample where the proper dilution factor is not known, the time scans of several different dilutions can be compared to determine the most accurate dilution within the acceptable

range of 200–2000. When comparing time scans, an inspection of the spacing between the car be compared to determine the most accurate dilution within the acceptable range of peak events in each dilution should be performed to ensure the most accurate results (Fig. 2002–2000). When comparing time scans, an inspection of the spacing between the peak events in each dilution should be performed to ensure the most accurate results (Figure 5).

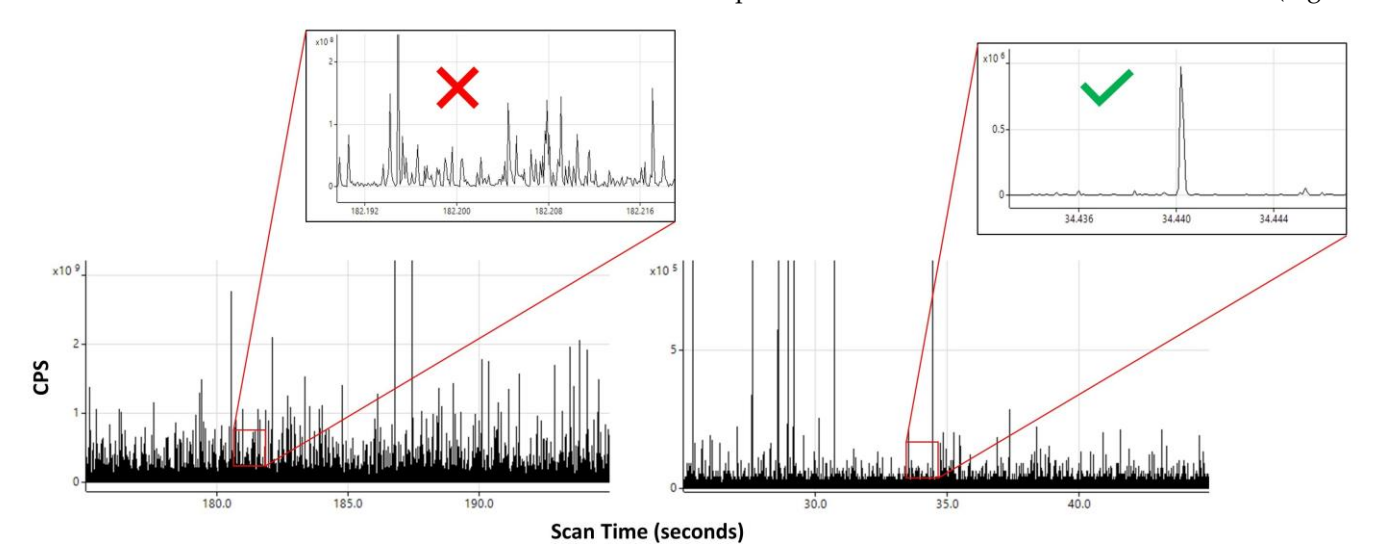


Figure 5. (Left): Time scan derived from spICP-MS/MS illustrating peak spacing issues arising from samples that are too concentrated within a 0.2 stime scan in counts per second (CPS) (inset): (Right): rom samples that are too concentrated within a 0.2 stime scan in counts per second (CPS) (inset): Peak spacing of a properly diluted sample within a 0.4 stime scan (inset). (Right): Peak spacing of a properly diluted sample within a 0.4 stime scan (inset).

When multiple elements are measured simultaneously, the evaluation of multiple dilution factors is especially important due to the variation in concentration across different elements. Furthermore, che evaluation of multiple dilution factors during an against serves asry stanica quality. Portex a libre saze also risk distribution is generally a wintaired with a concernent degreese in particle count proportional to the callution of charles illustrately an trates pre example of chilutis of facts on sparticle sparticle accounts and their vesnective dilution entimorphes Monrasont in applic pample Carticle court of particles evere abserved in the first four, dilutions etherefore it helikelihend of multiple particle events of nagticle and resetioned encesed the confidence in the date. The larger zero tick in the larger zero the larger for with luter rowith are 2000 pasticles existable of axplained by storbeth rectine describing the later than the control of the contro oranje siderina se se il dell'atte dell'attendo della la cuit della se il della contra della con capted to transitions can go which must by the propositioned dysthe appropriate to dark east ive portiel diamon refetive et unbardibution e Perfuel biocarity sin than particle downtlanio functions difficultifutionierationie difficultate ofchiene gleve it that leaf Cof troobogened tin intathe of Certed observed in datation letted from the chirt did not an detal as to make the comment of the comments of the comm dilution contions melasi per dont singilution ratio seems promising.

Table 9. Quantitative results for manganese (assumed chemical composition: MnO_2) in consecutive dilutions of an eyeshadow powder:

Dilution	Most Frequent Size Minition	Most Frequent Average Size (nm) Size (nm)	Average Size Partiele Count	Particle Qualitya of the Sults
1:1	70 —	83	(nm) 6837	Count
1:3	64 1:1	77 70	83866	6837 _{Too} many particles; high
1:7	60	71	4263	dissolved content
1:15	54 1:3	$64 \ 64$	<i>7</i> 2977	5000
1:31	52	61	_1570	cles; high dissolved 4263 Good particle range content
1:63	52 1:7	62 60	7_{828}	4263 Good particle range content
	1:15	54	64	2977
	3.5. Matrix Mato 1:31	ching 52	61	1570

A common issue faced in spICP-MS research is the lack of certified reference materials available in various matrices. Unfortunately, this makes it difficult to account for the

A common issue faced in spICP-MS research is the lack of certified reference materials available in various matrices. Unfortunately, this makes it difficult to account for the matrix effects to the full extent. One validation technique that has been proposed in the use of spiked samples [59]. In this approach, NPs of known size and composition are added to the sample matrix and the recovery of the spiked NPs is evaluated. Ideally, the recovery of the added mass should be assessed along with any variability in particle size matrix effects to the full extent. One validation technique that has been proposed is the and distribution [60]. Table 10 lists the values for particle count. NPC, mass concentration, use of spiked samples [59]. In this approach, NPs of known size and composition are and average mean size for a matrix free reference material (RM), a spiked FC sample and the recovery of the spiked NPs is evaluated. Ideally, the an unspiked FC sample. The recovery percentages for the NPC and mass concentration recovery of the added mass should be assessed along with any variability in particle size were 37-193% and [101-105]. Table, to lists the Values for particle count, NPC, mass concentration, and average mean size for a matrix-free reference material (RM), a spiked FC sample, and Table 10. Particle count and mean size data obtained from spiking experiment. an unspiked FC sample. The recovery percentages for the NFC and mass concentration were 92–95% and 101–105%, respectively. Sample Treatment

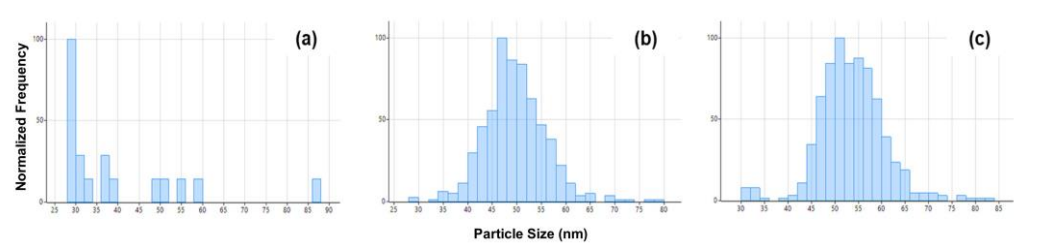
Table 10. Particle count and mean rize data obtain	ned from spiking experiment.	51 + 1

		*
Sample Tresmiend FC Sample		Mean Size [†] (1m)
Matrix Free Fishiked FC Sample	513 ± 30 19 ± 8	₅₁ 42 ± 5
Spiked FC Sample	478 ± 21	52 ± 1
Unspiked FC Sample	19 ± 8	42 ± 5

Particle Count

Mean Size (nm)

Figure 6 illustrates the size distribution histograms for each unspiked FC sample (Figure 84), maillustreet and prize etist, ibution keist per progresses da see sike de Est canade nfeignisezea) amatrix-free RMnfeignre size and roiked Fickfigrum et a Based conthe calculated veranties and nitomparies 2 outserization; tib valuation abit opin me than our set out there was very little variability in the size distribution, as validated with the high % recovery.



Ffigure66 Particlessized distributions for 4a husppiked FC sample (b) maatrix free RM and (c) spiked FECsaannpble.

Thoughthis approach attempts to evaluate the technique's ability to overcome entix teffects, the enseenf. NF arionic content at the came campo eiting as that spiking apaterial ria the apikerlo apir leuram fail travimir the true condition continue of the market burner is the traville that is the condition of the continue of the conti cassed of the spiked, Fine appleed or trained previous and person of Algorithms (iening of Algorithms) while this NTRY, froilitetethstterace grunnace is ulations, this is nata universal approach and it crum of be papatie, and it Narrom be stip me present in a sample slde ally a certified a stample. The target of ceach elle semposition evolud be remplexed for nospiked a melle study a hor respiked stiffed preference materials remain unavailable for use in spICP-MS.

3.6. Addressing the Challenges and Limitations of Screening NPs in FCs Using spICP-MS/MS 3.6. Addressing the Challenges and Limitations of Screening NPs in FCs Using spICP-MS/MS Single-particle ICP-MS/MS is a fairly recent analytical technique that is still undergoing development. That said, there are many challenges and limitations that need to be considered. A major challenge for spICP-MS/MS applications is the lack of commercing development of the considered of the conside products. For this reason, it is difficult to fully understand the effect of complex matrices and data derived from spICP-MS/MS analyses. Dilutions minimize matrix effects but cannot eliminate them entirely. In addition, maintaining particle stability and suspension is difficult in complex matrices where high ionic concentrations may negatively impact the results. For example, particles will settle over time during sample analysis, leading to possible inconsistencies in the particle count. Quantitative spICP-MS analysis has proven to be difficult when analyzing high-matrix samples. The elevated background may overlap with particle distributions, producing an unreliable truncated size distribution, and is dependent on the threshold detection limit (Figure 2). As mentioned, efforts to reduce elevated background include the utilization of microsecond dwell time [61], multiple sample

Nanomaterials **2023**, 13, 2681 14 of 17

dilutions, and tandem mass spectrometry to reduce spectral interferences. Despite utilizing these techniques, the ionic background was still often indistinguishable from the particle distribution; therefore, only qualitative and semi-quantitative results are presented.

4. Conclusions

An spICP-MS/MS screening method was successfully developed and applied to simultaneously identify nine different NP compositions in FC products purchased in the United States. The results from this study provide a fast, routine method using spICP-MS/MS for the screening of NPs in FC products. There were no clear trends observed between price, color, application (eyeshadow, blush, or face powder), buzzword (vegan or organic), and appearance (matte or shimmer). However, every FC sample contained NPs that were not disclosed on its ingredient list. The FDA regulates cosmetic products sold in the U.S.; however, at this time, there are no regulations addressing the use of NPs or the disclosure of NPs on packaging. Further, the use of buzzwords commonly found on cosmetic packaging may lead to the assumption that a product is nontoxic, which is misleading to health-conscious consumers given the potential for NPs to negatively impact human health and the environment.

Supplementary Materials: The following supporting information can be downloaded at https://www.mdpi.com/article/10.3390/nano13192681/s1, Figure S1. Time scans are shown for the nine analyzed elements in Sample A.; Figure S2. Time scans are shown for the nine analyzed elements in Sample C; Figure S4. Time scans are shown for the nine analyzed elements in Sample D; Figure S5. Time scans are shown for the nine analyzed elements in Sample E; Figure S6. Time scans are shown for the nine analyzed elements in Sample F; Figure S7. Time scans are shown for the nine analyzed elements in Sample G; Figure S8. Time scans are shown for the nine analyzed elements in Sample G; Figure S9. Transmission electron microscopy illustrating the presence of many nanoparticles less than 100 nm for Sample G.

Author Contributions: Conceptualization, D.H., J.N. and P.Z.; methodology, D.H. and J.N.; software, D.H. and J.N.; validation, D.H.; formal analysis, D.H.; investigation, D.H. and B.N.D.; resources, P.Z.; data curation, D.H. and J.N.; writing—original draft preparation, D.H.; writing—review and editing, D.H., J.N. and P.Z.; visualization, D.H. and J.N.; supervision, P.Z.; project administration, P.Z.; funding acquisition, P.Z. All authors have read and agreed to the published version of the manuscript.

Funding: DH was funded by LA Board of Reagents LEQSF(2020-23)-RD-A-31. ICP-MS/MS was awarded through NSF MRI CHE2018417 (PZ). This work was partially funded by the National Academies of Science, Engineering, and Medicine Gulf Research Program Early-Career Fellowship (PZ).

Data Availability Statement: Data are contained within the article or Supplementary Material.

Acknowledgments: The authors would like to thank Mark Kelinske at Agilent Technologies for his constant support and expertise. EDS support was provided by Mark Granier.

Conflicts of Interest: The authors declare no conflict of interest. The funders had no role in the design of the study; in the collection, analyses, or interpretation of data; in the writing of the manuscript; or in the decision to publish the results.

References

- 1. Maamoun, A. The Cosmetics Industry in the 2020s: A Case Study. Glob. J. Bus. Pedagog. Vol. 2022, 6.
- 2. Amberg, N.; Fogarassy, C. Green Consumer Behavior in the Cosmetics Market. Resources 2019, 8, 137. [CrossRef]
- 3. Whitehead, H.D.; Venier, M.; Wu, Y.; Eastman, E.; Urbanik, S.; Diamond, M.L.; Shalin, A.; Schwartz-Narbonne, H.; Bruton, T.A.; Blum, A.; et al. Fluorinated Compounds in North American Cosmetics. *Environ. Sci. Technol. Lett.* **2021**, *8*, 538–544. [CrossRef]
- 4. Lin, Y.; Yang, S.; Hanifah, H.; Iqbal, Q. An Exploratory Study of Consumer Attitudes toward Green Cosmetics in the UK Market. *Adm. Sci.* **2018**, *8*, 71. [CrossRef]
- 5. Lorenz, C.; Von Goetz, N.; Scheringer, M.; Wormuth, M.; Hungerbühler, K. Potential exposure of German consumers to engineered nanoparticles in cosmetics and personal care products. *Nanotoxicology* **2010**, *5*, 12–29. [CrossRef]

Nanomaterials **2023**, 13, 2681 15 of 17

6. Bilal, M.; Mehmood, S.; Iqbal, H.M.N. The Beast of Beauty: Environmental and Health Concerns of Toxic Components in Cosmetics. *Cosmetics* **2020**, *7*, 13. [CrossRef]

- 7. Baki, G. Introduction to Cosmetic Formulation and Technology; John Wiley & Sons: Hoboken, NJ, USA, 2022.
- 8. Color Additives History. Available online: https://www.fda.gov/industry/color-additives/color-additives-history (accessed on 3 August 2023).
- 9. Giles, R.E. The Fair Packaging and Labeling Act of 1966. Food Drug Cosmet. Law J. 1967, 22, 169–176.
- 10. Weir, A.; Westerhoff, P.; Fabricius, L.; Hristovski, K.; von Goetz, N. Titanium Dioxide Nanoparticles in Food and Personal Care Products. *Environ. Sci. Technol.* **2012**, *46*, 2242–2250. [CrossRef]
- 11. Gupta, V.; Mohapatra, S.; Mishra, H.; Farooq, U.; Kumar, K.; Ansari, M.J.; Aldawsari, M.F.; Alalaiwe, A.S.; Mirza, M.A.; Iqbal, Z. Nanotechnology in Cosmetics and Cosmeceuticals—A Review of Latest Advancements. *Gels* **2022**, *8*, 173. [CrossRef]
- 12. Mihranyan, A.; Ferraz, N.; Strømme, M. Current status and future prospects of nanotechnology in cosmetics. *Prog. Mater. Sci.* **2012**, *57*, 875–910. [CrossRef]
- 13. Lu, P.J.; Cheng, W.L.; Huang, S.C.; Chen, Y.P.; Chou, H.K.; Cheng, H.F. Characterizing titanium dioxide and zinc oxide nanoparticles in sunscreen spray. *Int. J. Cosmet. Sci.* **2015**, 37, 620–626. [CrossRef] [PubMed]
- Lu, P.J.; Fang, S.W.; Cheng, W.L.; Huang, S.C.; Huang, M.C.; Cheng, H.F. Characterization of titanium dioxide and zinc oxide nanoparticles in sunscreen powder by comparing different measurement methods. *J. Food Drug Anal.* 2018, 26, 1192–1200. [CrossRef] [PubMed]
- 15. Lu, P.-J.; Huang, S.-C.; Chen, Y.-P.; Chiueh, L.-C.; Shih, D.Y.-C. Analysis of titanium dioxide and zinc oxide nanoparticles in cosmetics. *J. Food Drug Anal.* **2015**, 23, 587–594. [CrossRef] [PubMed]
- 16. Corinaldesi, C.; Marcellini, F.; Nepote, E.; Damiani, E.; Danovaro, R. Impact of inorganic UV filters contained in sunscreen products on tropical stony corals (*Acropora* spp.). *Sci. Total Environ.* **2018**, *637–638*, 1279–1285. [CrossRef] [PubMed]
- 17. Hubbs, A.F.; Mercer, R.R.; Benkovic, S.A.; Harkema, J.; Sriram, K.; Schwegler-Berry, D.; Goravanahally, M.P.; Nurkiewicz, T.R.; Castranova, V.; Sargent, L.M. Nanotoxicology—A Pathologist's Perspective. *Toxicol. Pathol.* **2010**, *39*, 301–324. [CrossRef]
- 18. Krug, H.F.; Wick, P. Nanotoxicology: An Interdisciplinary Challenge. Angew. Chem. Int. Ed. 2011, 50, 1260–1278. [CrossRef]
- 19. Warheit, D.B.; Sayes, C.M.; Reed, K.L.; Swain, K.A. Health effects related to nanoparticle exposures: Environmental, health and safety considerations for assessing hazards and risks. *Pharmacol. Ther.* **2008**, *120*, 35–42. [CrossRef]
- 20. Zhang, J.; Guo, W.; Li, Q.; Wang, Z.; Liu, S. The effects and the potential mechanism of environmental transformation of metal nanoparticles on their toxicity in organisms. *Environ. Sci. Nano* **2018**, *5*, 2482–2499. [CrossRef]
- 21. Sharma, V.K. Aggregation and toxicity of titanium dioxide nanoparticles in aquatic environment—A Review. *J. Environ. Sci. Health Part A* **2009**, *44*, 1485–1495. [CrossRef]
- 22. Review of the EPA's Draft Fifth Contaminant Candidate List (CCL 5). Available online: https://sab.epa.gov/ords/sab/f?p=100: 18:14475496335862:::18:P18_ID:2600#report. (accessed on 13 August 2023).
- 23. Regulation (EC) No 1223/2009 of the European Parliament and of the Council of 30 November 2009 on Cosmetic Products. Available online: https://eur-lex.europa.eu/legal-content/EN/TXT/?uri=CELEX%3A02009R1223-20221217 (accessed on 3 August 2023).
- 24. Bundschuh, M.; Filser, J.; Lüderwald, S.; McKee, M.S.; Metreveli, G.; Schaumann, G.E.; Schulz, R.; Wagner, S. Nanoparticles in the Environment: Where Do We Come From, Where Do We Go To? *Environ. Sci. Eur.* **2018**, *30*, 6. [CrossRef]
- 25. Aiken, G.R.; Hsu-Kim, H.; Ryan, J.N. Influence of Dissolved Organic Matter on the Environmental Fate of Metals, Nanoparticles, and Colloids. *Environ. Sci. Technol.* **2011**, *45*, 3196–3201. [CrossRef] [PubMed]
- 26. Domingos, R.F.; Tufenkji, N.; Wilkinson, K.J. Aggregation of Titanium Dioxide Nanoparticles: Role of a Fulvic Acid. *Environ. Sci. Technol.* **2009**, 43, 1282–1286. [CrossRef] [PubMed]
- 27. Johnson, R.L.; Johnson, G.O.; Nurmi, J.T.; Tratnyek, P.G. Natural Organic Matter Enhanced Mobility of Nano Zerovalent Iron. *Environ. Sci. Technol.* **2009**, 43, 5455–5460. [CrossRef] [PubMed]
- 28. Yu, S.; Liu, J.; Yin, Y.; Shen, M. Interactions between engineered nanoparticles and dissolved organic matter: A review on mechanisms and environmental effects. *J. Environ. Sci.* **2018**, *63*, 198–217. [CrossRef] [PubMed]
- 29. Tan, C.; Fan, W.-H.; Wang, W.-X. Role of Titanium Dioxide Nanoparticles in the Elevated Uptake and Retention of Cadmium and Zinc in *Daphnia magna*. *Environ. Sci. Technol.* **2011**, *46*, 469–476. [CrossRef]
- 30. Mei, N.; Hedberg, J.; Ekvall, M.T.; Kelpsiene, E.; Hansson, L.-A.; Cedervall, T.; Blomberg, E.; Odnevall, I. Transfer of Cobalt Nanoparticles in a Simplified Food Web: From Algae to Zooplankton to Fish. *Appl. Nano* **2021**, *2*, 184–205. [CrossRef]
- 31. Tangaa, S.R.; Selck, H.; Winther-Nielsen, M.; Khan, F.R. Trophic transfer of metal-based nanoparticles in aquatic environments: A review and recommendations for future research focus. *Environ. Sci. Nano* **2016**, *3*, 966–981. [CrossRef]
- 32. NHepp, M.; Mindak, W.R.; Gasper, J.W.; Thompson, C.B.; Barrows, J.N. Survey of cosmetics for arsenic, cadmium, chromium, cobalt, lead, mercury, and nickel content. *J. Cosmet. Sci.* **2014**, *65*, 125–145.
- 33. Bocca, B.; Forte, G.; Pino, A.; Alimonti, A. Heavy metals in powder-based cosmetics quantified by ICP-MS: An approach for estimating measurement uncertainty. *Anal. Methods* **2012**, *5*, 402–408. [CrossRef]
- 34. Pawlaczyk, A.; Gajek, M.; Balcerek, M.; Szynkowska-Jóźwik, M.I. Determination of Metallic Impurities by ICP-MS Technique in Eyeshadows Purchased in Poland. Part I. *Molecules* **2021**, *26*, 6753. [CrossRef]
- 35. Vidmar, J.; Hässmann, L.; Loeschner, K. Single-Particle ICP–MS as a Screening Technique for the Presence of Potential Inorganic Nanoparticles in Food. *J. Agric. Food Chem.* **2021**, *69*, 9979–9990. [CrossRef] [PubMed]

Nanomaterials **2023**, 13, 2681 16 of 17

36. Candás-Zapico, S.; Kutscher, D.; Montes-Bayón, M.; Bettmer, J. Single particle analysis of TiO2 in candy products using triple quadrupole ICP-MS. *Talanta* **2018**, *180*, 309–315. [CrossRef] [PubMed]

- 37. Mansor, M.; Drabesch, S.; Bayer, T.; Van Le, A.; Chauhan, A.; Schmidtmann, J.; Peiffer, S.; Kappler, A. Application of Single-Particle ICP-MS to Determine the Mass Distribution and Number Concentrations of Environmental Nanoparticles and Colloids. *Environ. Sci. Technol. Lett.* **2021**, *8*, 589–595. [CrossRef]
- 38. Peters, R.J.B.; van Bemmel, G.; Herrera-Rivera, Z.; Helsper, H.P.F.G.; Marvin, H.J.P.; Weigel, S.; Tromp, P.C.; Oomen, A.G.; Rietveld, A.G.; Bouwmeester, H. Characterization of Titanium Dioxide Nanoparticles in Food Products: Analytical Methods To Define Nanoparticles. *J. Agric. Food Chem.* **2014**, *62*, 6285–6293. [CrossRef]
- 39. de la Calle, I.; Menta, M.; Klein, M.; Séby, F. Screening of TiO₂ and Au nanoparticles in cosmetics and determination of elemental impurities by multiple techniques (DLS, SP-ICP-MS, ICP-MS and ICP-OES). *Talanta* **2017**, *171*, 291–306. [CrossRef]
- 40. Balcaen, L.; Bolea-Fernandez, E.; Resano, M.; Vanhaecke, F. Inductively coupled plasma—Tandem mass spectrometry (ICP-MS/MS): A powerful and universal tool for the interference-free determination of (ultra)trace elements—A tutorial review. *Anal. Chim. Acta* 2015, 894, 7–19. [CrossRef]
- 41. Pace, H.E.; Rogers, N.J.; Jarolimek, C.; Coleman, V.A.; Higgins, C.P.; Ranville, J.F. Determining Transport Efficiency for the Purpose of Counting and Sizing Nanoparticles via Single Particle Inductively Coupled Plasma Mass Spectrometry. *Anal. Chem.* **2011**, *83*, 9361–9369. [CrossRef]
- 42. Haynes, W.M.; Lide, D.R.; Bruno, T.J. (Eds.) CRC Handbook of Chemistry and Physics, 94th ed.; CRC Press: Boca Raton, FL, USA, 2013.
- 43. Laborda, F.; Gimenez-Ingalaturre, A.C.; Bolea, E.; Castillo, J.R. Single particle inductively coupled plasma mass spectrometry as screening tool for detection of particles. *Spectrochim. Acta Part B At. Spectrosc.* **2019**, *159*, 105654. [CrossRef]
- 44. Mozhayeva, D.; Engelhard, C. A quantitative nanoparticle extraction method for microsecond time resolved single-particle ICP-MS data in the presence of a high background. *J. Anal. At. Spectrom.* **2019**, *34*, 1571–1580. [CrossRef]
- 45. Schwertfeger, D.M.; Velicogna, J.R.; Jesmer, A.H.; Scroggins, R.P.; Princz, J.I. Single Particle-Inductively Coupled Plasma Mass Spectroscopy Analysis of Metallic Nanoparticles in Environmental Samples with Large Dissolved Analyte Fractions. *Anal. Chem.* **2016**, *88*, 9908–9914. [CrossRef]
- 46. Gimenez-Ingalaturre, A.C.; Ben-Jeddou, K.; Perez-Arantegui, J.; Jimenez, M.S.; Bolea, E.; Laborda, F. How to trust size distributions obtained by single particle inductively coupled plasma mass spectrometry analysis. *Anal. Bioanal. Chem.* **2022**, 415, 2101–2112. [CrossRef] [PubMed]
- 47. Sanajou, S.; Şahin, G.; Baydar, T. Aluminium in cosmetics and personal care products. *J. Appl. Toxicol.* **2021**, 41, 1704–1718. [CrossRef] [PubMed]
- 48. Kokura, S.; Handa, O.; Takagi, T.; Ishikawa, T.; Naito, Y.; Yoshikawa, T. Silver nanoparticles as a safe preservative for use in cosmetics. *Nanomed. Nanotechnol. Biol. Med.* **2010**, *6*, 570–574. [CrossRef]
- 49. Bandura, D.R.; Baranov, V.I.; Tanner, S.D. Reaction chemistry and collisional processes in multipole devices for resolving isobaric interferences in ICP–MS. *Anal. Bioanal. Chem.* **2001**, *370*, 454–470. [CrossRef]
- 50. Bolea-Fernandez, E.; Balcaen, L.; Resano, M.; Vanhaecke, F. Overcoming spectral overlap via inductively coupled plasma-tandem mass spectrometry (ICP-MS/MS). A tutorial review. *J. Anal. At. Spectrom.* **2017**, 32, 1660–1679. [CrossRef]
- 51. Sugiyama, N.; Shikamori, Y. Removal of spectral interferences on noble metal elements using MS/MS reaction cell mode of a triple quadrupole ICP-MS. *J. Anal. At. Spectrom.* **2015**, *30*, 2481–2487. [CrossRef]
- 52. Walkner, C.; Gratzer, R.; Meisel, T.; Bokhari, S.N.H. Multi-element analysis of crude oils using ICP-QQQ-MS. *Org. Geochem.* **2017**, 103, 22–30. [CrossRef]
- 53. Harouaka, K.; Hoppe, E.W.; Arnquist, I.J. A novel method for measuring ultra-trace levels of U and Th in Au, Pt, Ir, and W matrices using ICP-QQQ-MS employing an O₂ reaction gas. *J. Anal. At. Spectrom.* **2020**, *35*, 2859–2866. [CrossRef]
- 54. Sugiyama, N. Direct Analysis of Ultratrace Rare Earth Elements in Environmental Waters by ICP-QQQ. In *ICP-QQQ Applications* in Geochemistry, Mineral Analysis, and Nuclear Science; Agilent Technologies: Santa Clara, CA, USA; p. 56.
- 55. Kálomista, I.; Kéri, A.; Galbács, G. On the applicability and performance of the single particle ICP-MS nano-dispersion characterization method in cases complicated by spectral interferences. *J. Anal. At. Spectrom.* **2016**, *31*, 1112–1122. [CrossRef]
- 56. Bolea-Fernandez, E.; Leite, D.; Rua-Ibarz, A.; Liu, T.; Woods, G.; Aramendia, M.; Resano, M.; Vanhaecke, F. On the effect of using collision/reaction cell (CRC) technology in single-particle ICP-mass spectrometry (SP-ICP-MS). *Anal. Chim. Acta* **2019**, 1077, 95–106. [CrossRef]
- 57. May, T.W.; Wiedmeyer, R.H. A table of polyatomic interferences in ICP-MS. At. Spectrosc. 1998, 19, 150–155.
- 58. Aznar, R.; Barahona, F.; Geiss, O.; Ponti, J.; Luis, T.J.; Barrero-Moreno, J. Quantification and size characterisation of silver nanoparticles in environmental aqueous samples and consumer products by single particle-ICPMS. *Talanta* **2017**, 175, 200–208. [CrossRef] [PubMed]
- 59. Linsinger, T.; Chaudhry, Q.; Dehalu, V.; Delahaut, P.; Dudkiewicz, A.; Grombe, R.; von der Kammer, F.; Larsen, E.; Legros, S.; Loeschner, K.; et al. Validation of methods for the detection and quantification of engineered nanoparticles in food. *Food Chem.* **2013**, *138*, 1959–1966. [CrossRef] [PubMed]

Nanomaterials **2023**, *13*, 2681 17 of 17

60. Bolea, E.; Jimenez, M.S.; Perez-Arantegui, J.; Vidal, J.C.; Bakir, M.; Ben-Jeddou, K.; Giménez, A.C.; Ojeda, D.; Trujillo, C.; Laborda, F. Analytical applications of single particle inductively coupled plasma mass spectrometry: A comprehensive and critical review. *Anal. Methods* **2021**, *13*, 2742–2795. [CrossRef] [PubMed]

61. Hineman, A.; Stephan, C. Effect of dwell time on single particle inductively coupled plasma mass spectrometry data acquisition quality. *J. Anal. At. Spectrom.* **2014**, 29, 1252–1257. [CrossRef]

Disclaimer/Publisher's Note: The statements, opinions and data contained in all publications are solely those of the individual author(s) and contributor(s) and not of MDPI and/or the editor(s). MDPI and/or the editor(s) disclaim responsibility for any injury to people or property resulting from any ideas, methods, instructions or products referred to in the content.